A 50-MHz, 12-MW INDUCTION LINAC CURRENT MODULATOR

E. E. Bowles (General Atomics, San Diego, CA)
W. C. Turner (Lawrence Livermore National Laboratory, Livermore, CA)

ABSTRACT

This paper describes a scheme to control the intrapulse energy variations of long pulse bursts of an induction linac. Analog control over the electron beam injector current is exercised in such a way that accelerator beam load variations compensate for thermal impedance variations of the accelerator cell ferrites. Circuit topology and test data are presented. The circuit uses 64 planar triodes to modulate the shunt impedance of two induction cells of the electron beam injector. Delayed feedback is used to apply a control signal to the modulator that varies the injector current to null the interpulse beam energy sweep at the linac output. The modulator exerts analog control over the top 5% of the beam current. It operates at a 60-ns pulse width and at up to a 0.1% duty factor.

INTRODUCTION

Induction linacs provide the high-current electron beams needed in high-gain free electron laser amplifiers. As progressively shorter wave length sources are developed, the energy slew restrictions on the output linac beam become more stringent. This has required an active method of intrapulse beam energy control to keep the output beam energy within the amplifier bandwidth. The energy variation to be controlled is a voltage droop caused by a time- and temperature-dependent magnetization, or leakage, current in the accelerator's ferrite cores. This droop is analogous to the voltage droop displayed in pulse transformers with constant load and source impedances.

Since the beam current represents a significant load to the pulse line driving the cell, it is possible to regulate the accelerator cell voltage by controlling the beam current. The voltage droop caused by the increasing magnetization current can be offset if an equal amount of current is simultaneously subtracted from the beam load. The sum of these two currents ($I_{beam} + I_{ferrite}$) then presents a constant load to the cell driver, and a constant voltage is produced across the cell gap. The injector current controller is designed to vary the beam current in precisely this manner.

Single modules of a prototype current controller based on this concept have already been built and tested at Lawrence Livermore National Laboratory (LLNL). The full prototype modulator assembly is currently being built and is expected to be placed on LLNL's High Average Power (HAP) injector in the winter of 1989.

THEORY OF OPERATION

A simplified schematic of an accelerator cell in Fig. 1 illustrates the idea. The pulsed power drive, represented by an ideal voltage source $2V_0$ and impedance Z_0, is loaded by the parallel combination of ferrite impedance Z_f and beam current source I_b. For simplicity, assume that the source impedance is constant because generalization to variable Z_0 is straightforward. Constant beam voltage V_c then requires that the sum of the parallel load currents be constant. This can be achieved by varying I_b to compensate for impedance variation. In practice, it is desirable to compensate for most of the ferrite impedance variation by passively compensating Z_0 and then actively controlling the beam current to reduce the residual variation of beam energy to tolerable limits. From the equivalent circuit in Fig. 1, variation of cell voltage is related to variations of beam current and ferrite impedance by

$$\begin{aligned} \Delta V_c &= -[Z_0/(1+Z_0/Z_f)] \times \Delta I_b \\ &\quad +[V_c/(1+Z_0/Z_f)] \times (Z_0/Z_f) \times (\Delta Z_f/Z_f) . \end{aligned} \quad (1)$$

If Z_f is held constant, Eq. (2) gives the magnitude of accelerating voltage variation that can be obtained by ΔI_b,

$$\Delta V_c = -(Z_0/(1+Z_0/Z_f)) \times \Delta I_b \ , \quad (2)$$

and the current variation required to correct an impedance variation ΔZ_f is given by

$$\Delta I_b = (V_c/Z_f) \times (\Delta Z_f/Z_f) \ . \quad (3)$$

The most effective method of varying the space charge limited current output of the injector is to vary the voltage applied across the anode-cathode gap. The voltage-current characteristic of the injector is

$$I = KV^p \quad p \sim \frac{3}{2} \text{ if } V << 1 \text{ MeV} \quad (4)$$

$$p \sim 1 \text{ if } V >> 1 \text{ MeV} \ .$$

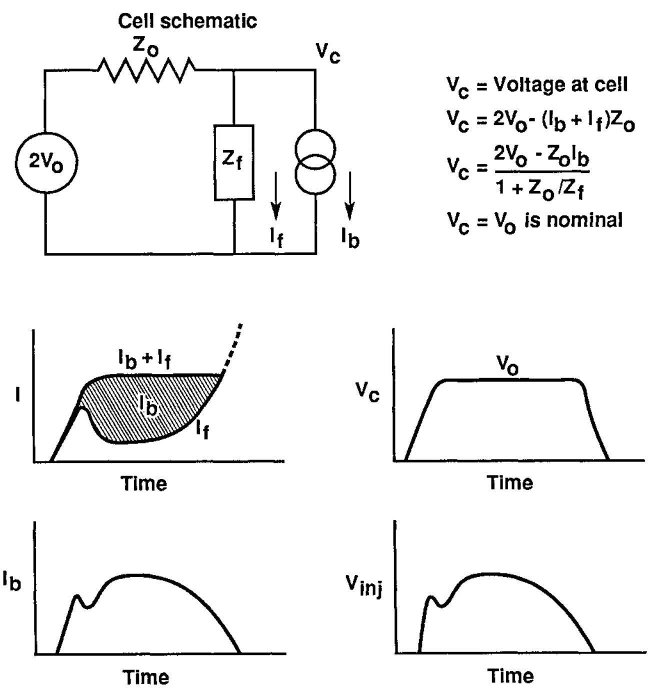

Fig. 1. Schematic of an accelerator cell.

Report Documentation Page

Form Approved
OMB No. 0704-0188

1. REPORT DATE	2. REPORT TYPE	3. DATES COVERED
JUN 1989	**N/A**	**-**

4. TITLE AND SUBTITLE
A 50-Mhz, 12-Mw Induction Linac Current Modulator

5a. CONTRACT NUMBER
5b. GRANT NUMBER
5c. PROGRAM ELEMENT NUMBER

6. AUTHOR(S)

5d. PROJECT NUMBER
5e. TASK NUMBER
5f. WORK UNIT NUMBER

7. PERFORMING ORGANIZATION NAME(S) AND ADDRESS(ES)
General Atomics, San Diego, CA

8. PERFORMING ORGANIZATION REPORT NUMBER

9. SPONSORING/MONITORING AGENCY NAME(S) AND ADDRESS(ES)

10. SPONSOR/MONITOR’S ACRONYM(S)

11. SPONSOR/MONITOR’S REPORT NUMBER(S)

12. DISTRIBUTION/AVAILABILITY STATEMENT
Approved for public release, distribution unlimited

13. SUPPLEMENTARY NOTES
See also ADM002371. 2013 IEEE Pulsed Power Conference, Digest of Technical Papers 1976-2013, and Abstracts of the 2013 IEEE International Conference on Plasma Science. Held in San Francisco, CA on 16-21 June 2013. U.S. Government or Federal Purpose Rights License.

14. ABSTRACT
This paper describes a scheme to control the intrapulse energy variations of long pulse bursts of an induction linac. Analog control over the electron beam injector current is exercised in such a way that accelerator beam load variations compensate for thermal impedance variations of the accelerator cell ferrites. Circuit topology and test data are presented. The circuit uses 64 planar triodes to modulate the shunt impedance of two induction cells of the electron beam injector. Delayed feedback is used to apply a control signal to the modulator that varies the injector current to null the interpulse beam energy sweep at the linac output. The modulator exerts analog control over the top 5% of the beam current. It operates at a 60-ns pulse width and at up to a 0.1% duty factor.

15. SUBJECT TERMS

16. SECURITY CLASSIFICATION OF:			17. LIMITATION OF ABSTRACT	18. NUMBER OF PAGES	19a. NAME OF RESPONSIBLE PERSON
a. REPORT	b. ABSTRACT	c. THIS PAGE			
unclassified	**unclassified**	**unclassified**	**SAR**	**4**	

LLNL's HAP injector, with a nominal output voltage of 1 MeV, is within the transition regime, and experimental data shows $p \sim 1.3$.

The injector is powered by two pulse lines charged to 200 kV. The difficulty in attempting to directly modulate such a high voltage has led to a different approach: two dedicated regulation cells are placed on the injector proper. The shunt impedance across each cell feed is modulated with a planar triode tube set to cause a voltage variation from 10–25 kV. The regulation cells, one on the anode and one on the cathode sides, modulate the injector voltage and therefore the current in relation to Eq. (4).

In an induction linac, each cell acts as a 1:1 pulse transformer. In a drive cell the current flowing into the cell feed is the primary current, and the beam current is the secondary current. In a regulation cell, however, the roles are reversed: the beam current is primary, and the current flowing through the regulation circuit is secondary.

Since the cell turn ratio is 1:1, a current equal to the beam current is induced in the regulation cell. If the burden resistance R_s (defined as $R_0 \parallel R_T$) applied across this constant current source is varied, the voltage drop across the cell will vary in direct proportion. The transconductance of the planar triode tube set in parallel with a fixed resistor provides this control. Figure 2 shows this arrangement.

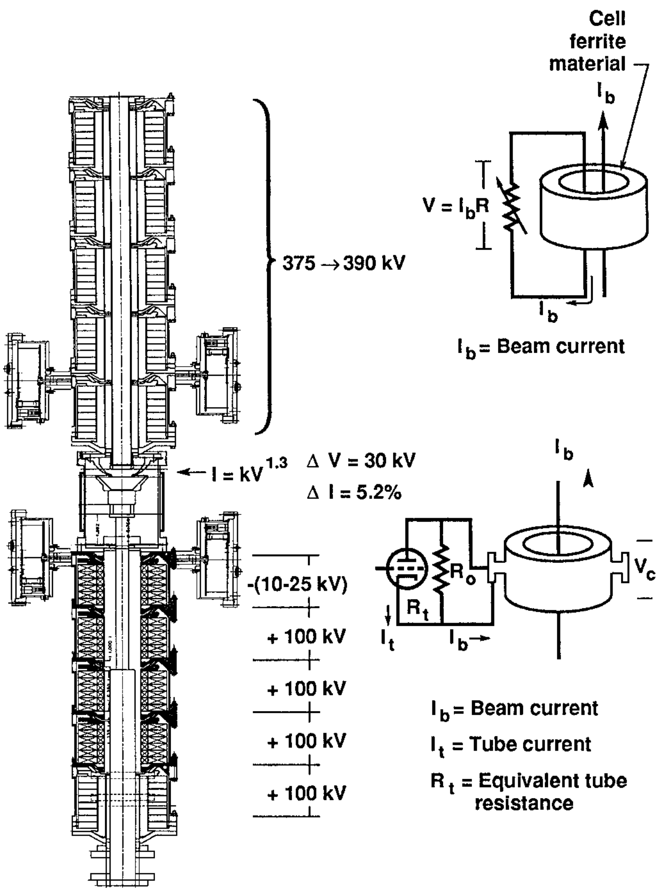

Fig. 2. Injector control concept, with the regulation cells shown on the injector at left.

Figure 3 is a block diagram of an accelerator with energy regulation by injector current control. An energy analyzer at the accelerator output digitizes and stores the beam energy variation $\Delta E(t)$ as a function of time. This signal is then summed with previous error signals, amplified, and applied to the injector current controller on the next pulse to give a compensating injector current variation

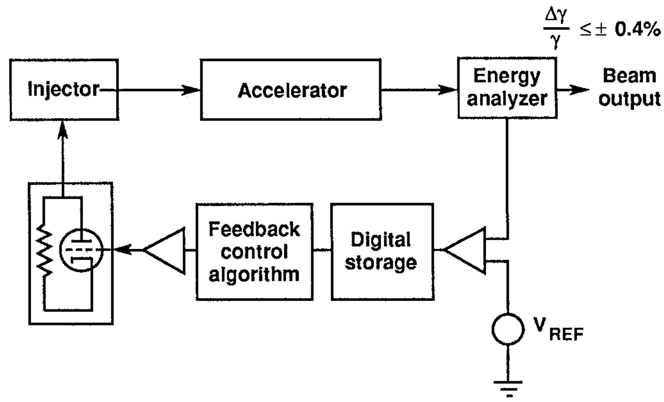

Fig. 3. Block diagram of an accelerator with energy regulation by injector current control.

$$\Delta I_b = -(1/Z_0 + 1/Z_f) \times (\Delta E/N) \ , \tag{5}$$

where N is the number of accelerator cells.

The maximum voltage swing in the diode is

$$\Delta V_{max} = \Delta R_s \times I_b = -30 \text{ kV} \ , \tag{6}$$

and the maximum current variation is

$$\Delta I_{b,max} = p \times I_b \times (\Delta V_{max}/V) \ . \tag{7}$$

For Eq. (7) we have assumed a p=1.3 power law for the current dependence on voltage, which is approximately true for V in the range of 0.8-1.5 MV. The nominal current for the injector is 800 A at a voltage of 800 kV. Solving for Eq. (7), $\Delta I_b = 39$ A = 0.05 I_b. The maximum power swing is 24 MW, or 12 MW per cell controller. For the case shown in Fig. 2, the polarity of the regulation cells and their cell reset is opposite that of the normal cells, and the tube cathodes are at ground potential, which is desirable from the viewpoint of the cathode heater circuit. It is possible for these cells to have the same polarity as the normal cells and cathode at ground if the order of ferrite and insulator is reversed (if normal cells are driven with negative polarity).

CIRCUIT DESCRIPTION

The regulator circuit is a coaxial array of 16 planar triode electron tubes in cascode connection with a microwave packaged field effect transistor (FET). The FET is driven by a 50-MHz wideband power operational amplifier with a 900-MHz bipolar radiofrequency (rf) transistor in an emitter follower configuration. Each tube is shunted by a 1000-Ω, 500-W resistor to provide a fixed value of maximum resistance and voltage.

Proper operation requires that the controller be as small as possible and be tightly coupled to the accelerator cell. The 25-kV prototype array to be tested on the HAP injector consists of a 16-tube coaxial array made up of 8 dual-tube modules. The tubes are placed in a 14-in-dia. × 7-in-tall freon-filled can that is directly connected to the accelerator cell. Controlled power density is > 10 kW/in^3. Figure 4 is a simplified single-module circuit schematic and assembled controller layout. Figure 5 shows a test circuit schematic and the input and output waveforms of a dual-tube module operating at the 500-kW level. The circuit performance exceeds our requirements.

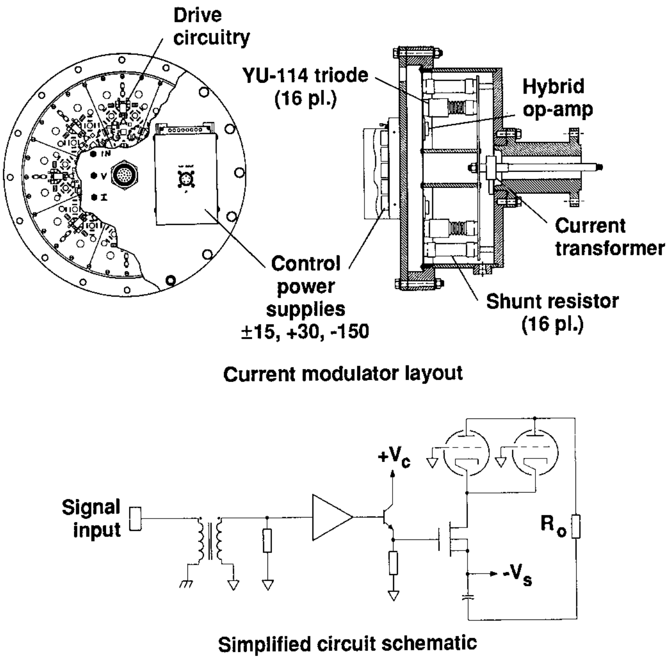

Fig. 4. Simplified schematic of a single-module circuit and assembled controller layout.

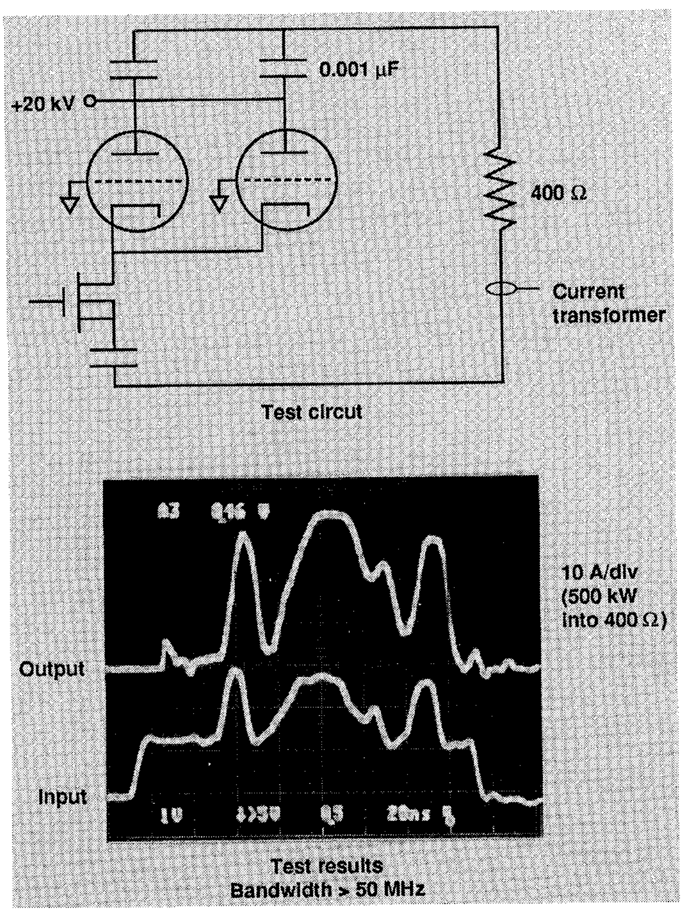

Fig. 5. Schematic of a test circuit and the input and output waveforms of a dual-tube module operating at the 500-kW level.

TRANSFER CHARACTERISTICS

The planar triode tube characteristics are shown in Fig. 6. As indicated, tube current is a function of grid bias and anode voltage.

The characteristic of the regulator circuit causes the anode voltage to fall rapidly as the tube current is increased. This and the maximum permissable grid bias cause the maximum obtainable current in the tube to be less than the emission limit of the cathode. Referring back to Fig. 1, the maximum obtainable current, and thus the maximum voltage swing, can be calculated in the following manner:

$$\begin{aligned} V_c &= (I_b - I_T)R_0 \\ I_T &= KV_c^{\frac{3}{2}} \\ V_c &= (I_b - KV_c^{\frac{3}{2}})R_0 \quad . \end{aligned}$$

The pertinent values for a 32-tube array of YU 114 tubes are

$$\begin{aligned} R &= 30\ \Omega \\ I_b &= 850\ \mathrm{A} \qquad \rightarrow V_c + .017V_c^{\frac{3}{2}} = 25,000 \\ K &= 5.6\times10^{-4}\ \mathrm{A}/V^{3/2} \end{aligned}$$

This equation can be solved by iteration:

V_c = 9,500 V = cell voltage minimum.
Cell voltage variation = 9.5→25kV.
I_T= 496 A or 15.5 A per tube.

The FET is a conductivity-modulated device which is essentially a voltage-controlled current source. The cascode connection of the FET automatically sets up grid bias (actually cathode depression) conditions on the tube to pass the amount of current that is commanded from the FET. The transfer characteristics of the tube-FET combination are shown in Fig. 7, along with the input-output characteristic of the entire current controller. This arrangement is particularly advantageous since it forces a linear V-I transfer characteristic on the tube output current, and it eliminates the auxiliary power supply and control circuitry that would be necessary to drive the tube into cutoff.

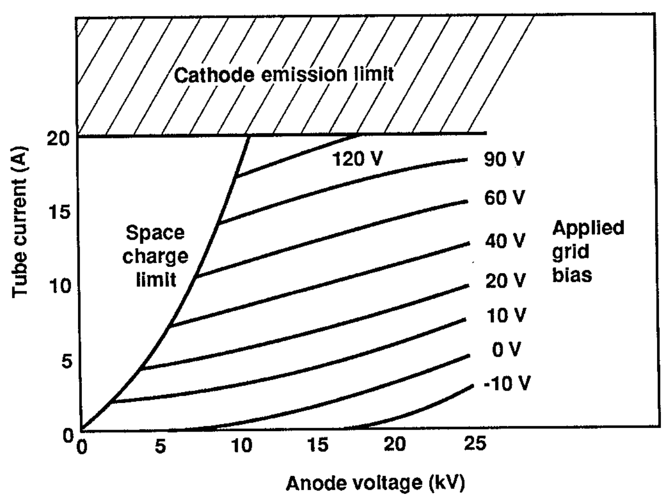

Fig. 6. Characteristics of an EIMAC YU 114 tube.

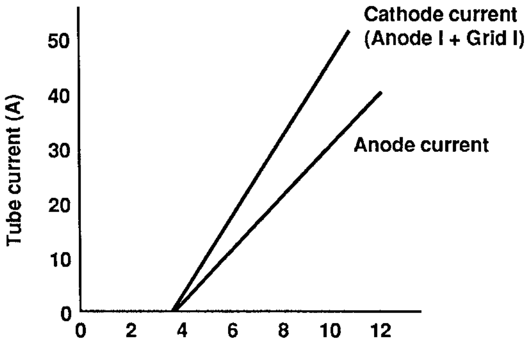

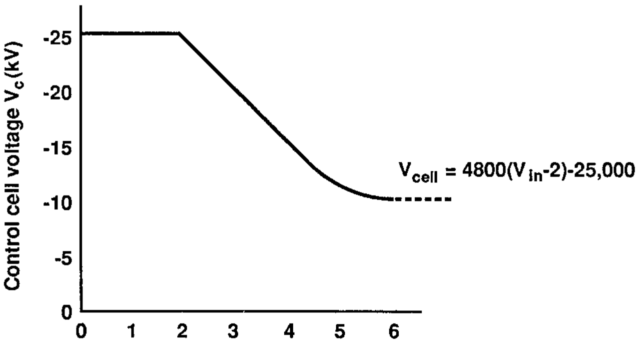

Fig. 7. Transfer characteristics of the tube-FET (top), and input-output characteristics of the entire current controller (bottom).

FEEDBACK LOOP

The current controller is intended to provide pulse-to-pulse feedback regulation of the beam energy. Figure 8 shows hardware implementation for the acquisition and processing of a feedback control signal. The feedback system must keep up with temperature-induced ferrite current variations. The beam energy analyzer acquires the error signal, and a microcomputer processes this signal and adds it to the current controller correction signal.

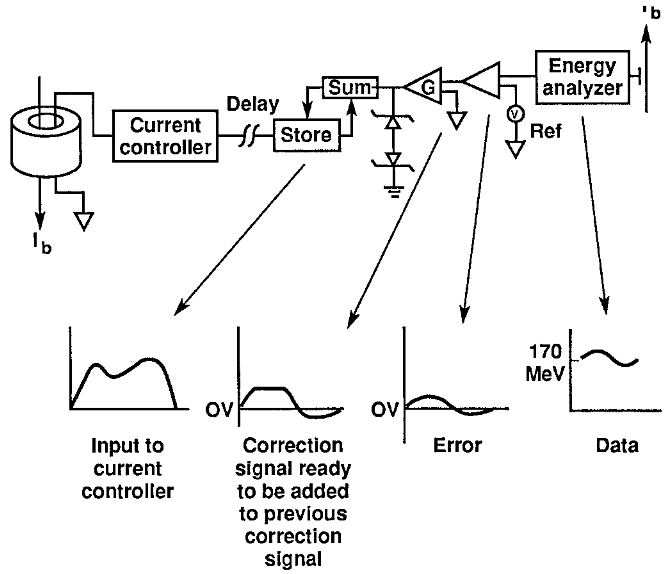

Fig. 8. Schematic of the feedback system.

The feedback control system is a single-feedback-loop sampled data control system. Since it is a sampled data system, the bandwidth is in terms of a number of pulses and must be high enough to compensate for temperature-induced ferrite variations. A high-speed transient digitizer is required to allow multiple waveforms to be acquired from the energy analyzer and to be ensemble-averaged to reduce measurement noise.

Before the feedback loop can be closed, the transfer function of the modulator, injector, accelerator, and energy analyzer must be measured. The transfer function is measured by applying various modulating waveforms to the current controller and by measuring the beam energy response function. After the transfer function is determined, the feedback algorithm is developed to provide a stable, well-defined system performance.

ACKNOWLEDGEMENT

This work was performed jointly under the auspices of the US DOE by LLNL under W-7405-ENG-48 and for the DOD under SDIO/SDC-ATC MIPR No. W31RPD-8-D5005.